Biogeosciences, 23, 4779–4791, 2026
https://doi.org/10.5194/bg-23-4779-2026

Biogeosciences Open Access EGU

Carbon accumulation in Mediterranean rhodolith beds during the Holocene

Silvia de Juan[1], Ryan Smazal[2], Claudio Lo Iacono[3], Maria del Mar Gil[1], Andrea Cabrito[3], Andres Ospina-Alvarez[1], Jorge Guillén[3], Grace M. Cott[2], Laia Illa-López[1], Hilmar Hinz[1], and Francesc Maynou[3]

[1]Instituto Mediterráneo de Estudios Avanzados IMEDEA (UIB-CSIC), c. Miquel Marquès 21, 07190 Esporles, Spain
[2]School of Biology and Environmental Science, University College Dublin, Dublin, Ireland
[3]Instituto de Ciencias del Mar (CSIC), Psg. Marítim de la Barceloneta 37-49, 08003 Barcelona, Spain

Correspondence: Silvia de Juan (silvia.dejuan@csic.es)

Received: 12 March 2026 – Discussion started: 18 March 2026
Revised: 3 June 2026 – Accepted: 30 June 2026 – Published: 9 July 2026

Abstract. Rhodolith and maërl beds are globally relevant biogenic ecosystems whose long-term carbon storage capacity remains poorly quantified, particularly in the Mediterranean. To fill this gap, we investigated the formation, structure, and carbon content of a sediment deposit underlying a rhodolith bed in the Menorca Channel (Western Mediterranean). High-resolution seismo-acoustic profiling revealed a highly heterogeneous biogenic sedimentary deposit at ∼ 60 m depth, with thickness ranging from a few centimeters to 3.7 m (mean = 0.95 m). Seven cores extracted from the thickest sediment deposits were analyzed for grain size, carbonate content, bioclast composition, organic carbon, and radiocarbon age. Radiocarbon dating indicates that sediment accumulation began during the early Holocene (11 700–9000 yr BP), when post-glacial sea-level rise transitioned the area from subaerial exposure to shallow-marine conditions. Despite the spatial limitation of collected data, several conclusions could be drawn. Early deposits produced during the last sea-level rise were dominated by bivalves and dispersed coralline fragments. The following establishment of modern sea level around 7000–6500 yr BP marks a change to the development of more stable dense rhodolith–maërl facies that persist today. Sediment accretion rates are low (median = 8.54 cm kyr^{-1}), reflecting very low external sediment supply, and slow growth of coralline algae. Organic carbon content in the upper 50 cm, representing the most dynamic and recently deposited carbon pool, averaged 0.57 % (±0.22), with an estimated organic carbon stock of 32.04 (±4.18) Mg C ha^{-1}. These results show that rhodolith beds can act as long-term organic carbon stores, forming spatially complex Holocene deposits that have been largely overlooked.

Highlights.

- Seismo-acoustic mapping of a deep rhodolith deposit revealed highly variable thickness.
- Holocene sedimentation began 11 700–9000 yr BP during post-glacial sea-level rise.
- Dense rhodolith–maërl facies formed after sea-level stabilization ∼ 7000 yr BP.
- Accretion rates are low (8.54 cm kyr^{-1}), very low external sediment supply and slow algal growth.
- Organic carbon averages 32.04 (±4.18) Mg C ha^{-1} in the upper 50 cm, of sediment.

1 Introduction

Marine ecosystems play an important role in the global carbon cycle by contributing to organic and inorganic carbon storage. Coastal systems sequester atmospheric carbon dioxide (CO_2) through photosynthesis and the subsequent burial of sedimentary organic carbon (Nellemann et al., 2009; Barbier et al., 2011). Current evidence suggests that net organic carbon burial in the marine environment comes from vegetated ecosystems such as mangroves, seagrass meadows and saltmarshes (Macreadie et al., 2019). In contrast, calcifying algal systems such as rhodolith and maërl beds have received considerably less attention, despite their global distri-

bution and the millennial persistence of their deposits. These characteristics suggests that they may represent an important, yet poorly quantified, long-term carbon store (Aguirre et al., 2017; Tuya et al., 2023; van der Heijden and Kamenos, 2015).

Rhodolith and maërl beds consist of free-living, non-geniculate calcareous red algae (Rhodophyta: *Corallinophycidae*) that form multi-specific assemblages in subtidal environments. These habitats typically occur on coarse mobile sediments under moderate hydrodynamic conditions that prevent burial while maintaining sufficient irradiance (Aguirre et al., 2017; Basso et al., 2017; Bosence, 1983). Despite their slow individual annual growth rates ($\sim 1\,\mathrm{mm\,yr^{-1}}$), rhodolith accumulations can reach several meters in thickness over hundreds to thousands of years. Living rhodoliths are restricted to the upper few centimeters of the bed, overlying deposits of fragmented coralline algae and skeletal remains of bryozoans, molluscs, and echinoderms (Fornós and Ahr, 1997; Betzler et al., 2011; Mao et al., 2020).

These long-lived carbonate-rich deposits may store carbon through both the accumulation of biogenic sediments and the trapping of organic carbon supplied from external sources (Mao et al., 2020; Schubert et al., 2024). The high particle-trapping capacity of rhodolith beds, driven by the three-dimensional structural complexity of the algae, is a key mechanism underpinning this process (Mao et al., 2020; James et al., 2024; Bulleri et al., 2025). This structure enhances the retention of suspended material, promoting the accumulation of organic material and supporting carbon cycling within detritus-based food-webs (Rendina et al., 2026). However, the broader role of rhodolith beds in carbon cycling remains uncertain, as carbon storage through particle retention simultaneously occurs with calcium carbonate production, a process that releases CO_2 (James et al., 2024; Mao et al., 2024). Thus, in carbonate-dominated systems, the balance between carbon burial and release of CO_2 is complex and not yet fully resolved (Macreadie et al., 2019). For the purposes of this study, we focus specifically on quantifying sedimentary organic carbon stocks and highlighting the potential for long-term storage, rather than resolving net ecosystem carbon balance.

Large rhodolith and maërl beds are present on modern and ancient carbonate shelves across tropical to polar regions (Riosmena-Rodríguez et al., 2017; Tuya et al., 2023), including the world's largest bed on the Brazilian continental shelf ($21\,000\,\mathrm{km^2}$, Amado-Filho et al., 2012). The Mediterranean hosts the second-largest bed described to date, covering approximately $470\,\mathrm{km^2}$ in the Menorca Channel, western Mediterranean (Tabone et al., 2024). Its development has been facilitated by the clear waters and low sediment input that characterize Mediterranean islands, allowing rhodolith beds to extend down to 90 m depth (Joher et al., 2016). Despite their ecological importance, the capacity of Mediterranean rhodolith beds to store sedimentary organic carbon over centennial to millennial timescales remains poorly quantified. This is particularly true for the vertical distribution and spatial variability of carbon stocks, as well as their relationship with deposit accretion history.

This knowledge gap is especially relevant given the high vulnerability of rhodolith beds to disturbance due to their slow growth and limited recovery capacity. These habitats are threatened by bottom-contact fishing gears, elevated suspended sediments, and the cumulative effects of ocean warming and acidification under climate change (Tuya et al., 2023; Trégarot et al., 2024). Although Mediterranean rhodolith beds are protected under EU Regulation 1997/2006, the EU Habitats Directive, and the UNEP-MAP-RAC/SPA Action Plan (2008), effective management remains limited due to insufficient spatial coverage and ecological data. Improving knowledge of their organic carbon storage capacity is essential not only to clarify their contribution to the global carbon cycle, but also to strengthen the scientific basis for conservation (de Macêdo Carneiro et al., 2021; Schubert et al., 2024).

This study quantifies the role of Mediterranean rhodolith beds in long-term organic carbon storage by analyzing sedimentary organic carbon deposition of a well-preserved deposit in the Menorca Channel (western Mediterranean). The Menorca Channel is a temperate carbonate shelf where rhodolith sediments have accumulated since the early Holocene, providing a unique archive to examine carbon storage over millennial timescales. Using high-resolution seismo-acoustic data, sediment cores and radiocarbon dating, we estimate the stock of organic carbon in the upper 50 cm of sediments. We test the hypothesis that this rhodolith bed represents a consistent Holocene carbon store, shaped by local environmental conditions and long-term sea-level changes, with implications for regional protection schemes for these habitats.

2 Material and methods

2.1 Study area

The Balearic continental shelf is a temperate, low-energy oligotrophic system dominated by carbonate-producing habitats, including *Posidonia oceanica* meadows, coralligenous communities, and extensive rhodolith–maërl beds (Canals and Ballesteros, 1997; Betzler et al., 2011). Our study focuses on the Menorca Channel, a shallow carbonate platform (~ 100 m max depth) between Mallorca and Menorca, where post-glacial neritic carbonates have accumulated since the early Holocene (Alonso et al., 1988; Betzler et al., 2011). Rhodolith and maërl beds occur between 45–80 m depth on the platform (Fig. 1), interspersed with detrital sands (de Juan et al., 2023). The preservation of these environments has been assisted by a historical trawling exclusion zone surrounding nearby submarine cables and, more recently, by the 2016 designation of the Menorca Channel as a Natura 2000 Site of Community Importance (SCI ESZZ16002).

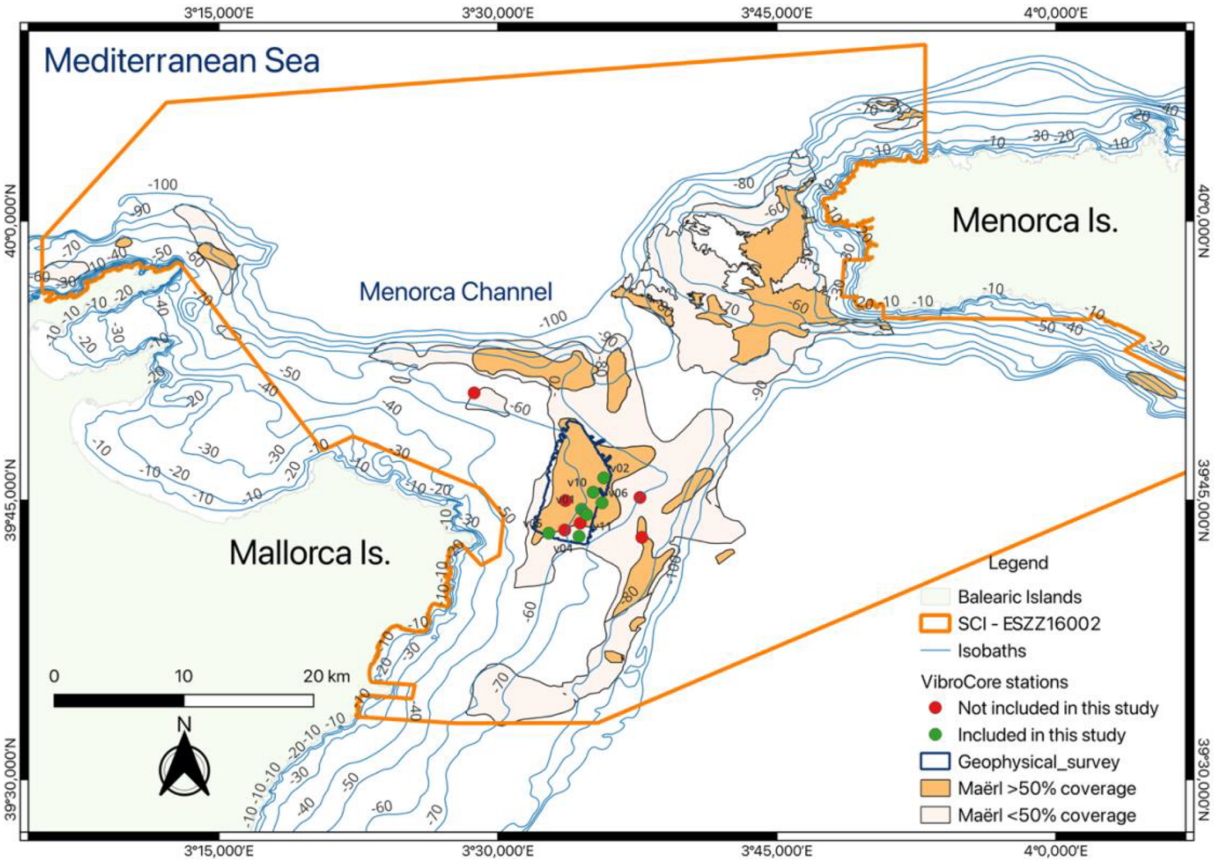

Figure 1. Study area in the Menorca Channel, located between Mallorca and Menorca islands in the western Mediterranean Sea. The map shows the area covered by the geophysical survey (dark blue polygon) and the location of VibroCore stations included (green dots) and not included (red dots) in this study. Rhodoliths are represented in light and dark orange, indicating areas with 10 %–50 % and > 50 % coverage, respectively. The Site of Community Importance (SCI ESZZ16002) is delineated by the dark orange boundary. Isobaths (in metres) are shown as blue contour lines. Source: modified from project INDEMARES (Moranta et al., 2014).

We focused on a 43.6 km^2 area where rhodolith and maërl cover exceeds 50 %, based on high-resolution mapping from the INDEMARES project (Moranta et al., 2014) and our own video surveys (Cabrito et al., 2024b). Within this area, we conducted high-resolution seismo-acoustic profiling to determine the thickness of bioclastic sediments above the acoustic basement and to identify suitable sites for recovering ≥ 1 m sediment corers. Potential sites were inspected with a remotely operated vehicle (ROV) to confirm rhodolith–maërl dominance, and full coverage was verified at all core locations.

2.2 Geophysical map

In May 2022, we acquired 56 high-resolution seismo-acoustic profiles in the study area (Fig. 1) during a research cruise aboard R/V *SOCIB* and using an INNOMAR Medium-100 non-linear parametric echosounder coupled with an INS SBG Navisight Ekinox and GNSS AtlasLink for positioning. Sound-speed and turbidity corrections were obtained with a Valeport SWIFT. The system emits two primary frequencies around 100 kHz, producing a secondary frequency of 5–12 kHz, with a pulse repetition rate of up to 30 s^{-1} and a beam width of $\pm 1.8°$. Non-linear parametric echosounders provide narrow, low-frequency beams with small footprints, enabling high-resolution imaging of shallow sediment deposits and precise localization of core-sampling (Lo Iacono et al., 2008).

Profiles were spaced 200 m apart, oriented NNE–SSW in the southern sector and NW–SE in the northern sector, intersected by perpendicular transversal profiles every 500–2000 m (Fig. S1 in the Supplement). Penetration depth averaged 0.8–1.0 m and reached a maximum of 3.7 m, maintaining high horizontal and vertical metric to sub-metric resolution due to the small pulse size. Uncertainties were estimated to be of the order of ± 0.2 m. Seismo-acoustic data were interpreted using INNOMAR-ISE 2.9 to pick stratigraphic horizons and estimate thickness of the bioclastic deposit. Geo-referencing and isopach mapping were conducted with Global Mapper and ArcGIS.

2.3 Sediment core sampling

In May 2023, sediment cores were collected at 60–80 m depth during a research cruise aboard R/V *Sarmiento de Gamboa*. The coring sites were selected based on geoacoustic evidence of maximum sediment thickness within the survey polygon (Fig. 2). A vibrocorer (ASTHER I, GEOMYTSA S.A.) operating at 136 kN centrifugal force at 3 m recovered 12 PVC-lined cores (9 cm diameter, 1.4–2.8 m length; Table 1). Each core was sectioned into ≤ 1 m segments and stored at -20 °C for laboratory analyses. Of the 12 cores, 7 were retained for this study; the remaining five cores were stored frozen for future genetic analysis to identify the presence of different species of rhodoliths (Fig. 1).

2.3.1 Sediment core opening and visual description

Each 1 m core section was cut longitudinally for analysis. All cores were visually inspected to describe sediment composition, and subsamples were collected for grain size, radiocarbon dating, bioclast identification, and organic carbon content analyses.

2.3.2 Grain size and carbonate contents

The cores were sampled at 5 cm intervals for grain-size and carbonate-content analyses. Grain-size distributions were measured using a HORIBA LA-950V2 laser diffraction analyser after disaggregating and removing the biogenic fraction (10 % H_2O_2), and ultrasonic dispersion; the > 2 mm fraction was quantified by sieving. We calculated the weight percentages of clay, silt, sand, and gravel, as well as mean grain size (ϕ), sorting (σ), skewness (Sk), and kurtosis (kG). Carbonate content was determined from the CO_2 volume displaced by a sample of sediment treated with 20 % HCl, calibrated against a 100 % $CaCO_3$ standard.

2.3.3 Radiocarbon dating

Between two and three bioclasts (rhodoliths or bivalve shells) from different depths in four cores (Table 1) were radiocarbon-dated by Beta Analytic (Miami, USA). Dates were calibrated with BetaCal 5.0, with HPD method "MARINE20" and corrected for the local marine reservoir effect ($\Delta R = -112 \pm 99$). Sediment accretion rates (cm kyr^{-1}) were calculated by dividing the thickness of sediment between successive dated horizons along the core (kyr), taking the top most horizon as 0 yr BP.

2.3.4 Taxonomic identification of bioclasts

Sediment was examined under a binocular microscope at ~ 50 cm intervals for fauna identification. Subsamples (10–20 g) were air-dried (48 h) and sieved through 0.5 and 1 mm meshes. Between 200 and 300 clasts from the > 0.5–1 mm and > 1 mm fractions were inspected and assigned to major taxonomic groups (Bivalves, Gastropods, Bryozoans, Echinoids, Foraminiferans, and free-living coralline algae). Rhodoliths were classified into two morphotypes following (Basso, 1998; Basso et al., 2012): non-branched rhodoliths (including "boxwork" and "praline" forms; 1–5 cm) and branched maërl fragments (0.5–2 cm) (see also Jardim et al., 2025; Teichert, 2024).

2.4 Organic Carbon Content

From each core, sediment samples (~ 21 mL) were collected using a syringe every 10 cm within the upper 50 cm, as this layer is expected to contain the highest and more dynamic carbon pool, which has not yet undergone long-term diagenesis (Middelburg, 2018). To minimize decomposition of organic matter and microbial growth, samples were kept cold (4 °C) during 24–48 h for later processing. In the laboratory, samples were weighed, freeze-dried (lyophilized) for 48–72 h, and weighed again to determine their moisture content percentage. Finally, the samples were finely ground in an agate ball mill.

The processed samples were sent to University College Dublin to be sub-sampled for further analysis. From each 10 cm layer, ~ 2.0 g (± 0.6 g) of homogenized sediment was subsampled for organic carbon (OC) analysis. A sub-set of the homogenized sample was then shipped to the University of Waterloo (Canada) for carbon and nitrogen analysis. The samples were analysed using an ECS 4010 Elemental Analyzer (NC Technologies, Italy) coupled to a Delta Plus XL (Thermo-Finnegan, Germany) continuous flow isotopic mass spectrometer (CRFIRMS). Samples were acid washed according to the University of Waterloo Environmental Isotope Laboratory procedures in order to remove inorganic carbon and obtain OC measurements. This included acid washing the sediments in HCl (10 mL of 10 %) for 24 h and until the reaction subsided. The final OC value was determined using the measured OC percentage of the acidified sample, which was normalized to the bulk sediment mass by multiplying by the samples non-carbonate fraction. High effervescence during acid treatment indicated a substantial carbonate fraction, resulting in a marked mass loss. The %C and %N was measured in bulk, analyzed against known certified elemental standard materials. For QA/QC, sample replicates were analyzed every 8 to 10 samples, with certified standard/reference materials comprising of at least 20 % of every run. Analytical control measures were based on the detection of major carbon (C) and nitrogen (N) peaks to ensure data consistency and calibration accuracy.

2.5 Data analysis

To evaluate whether sediment characteristics control the density of retained OC, variation in OC density (g cm^{-3}) was analysed in relation to sediment characteristics using linear mixed-effects models to account for the hierarchical structure

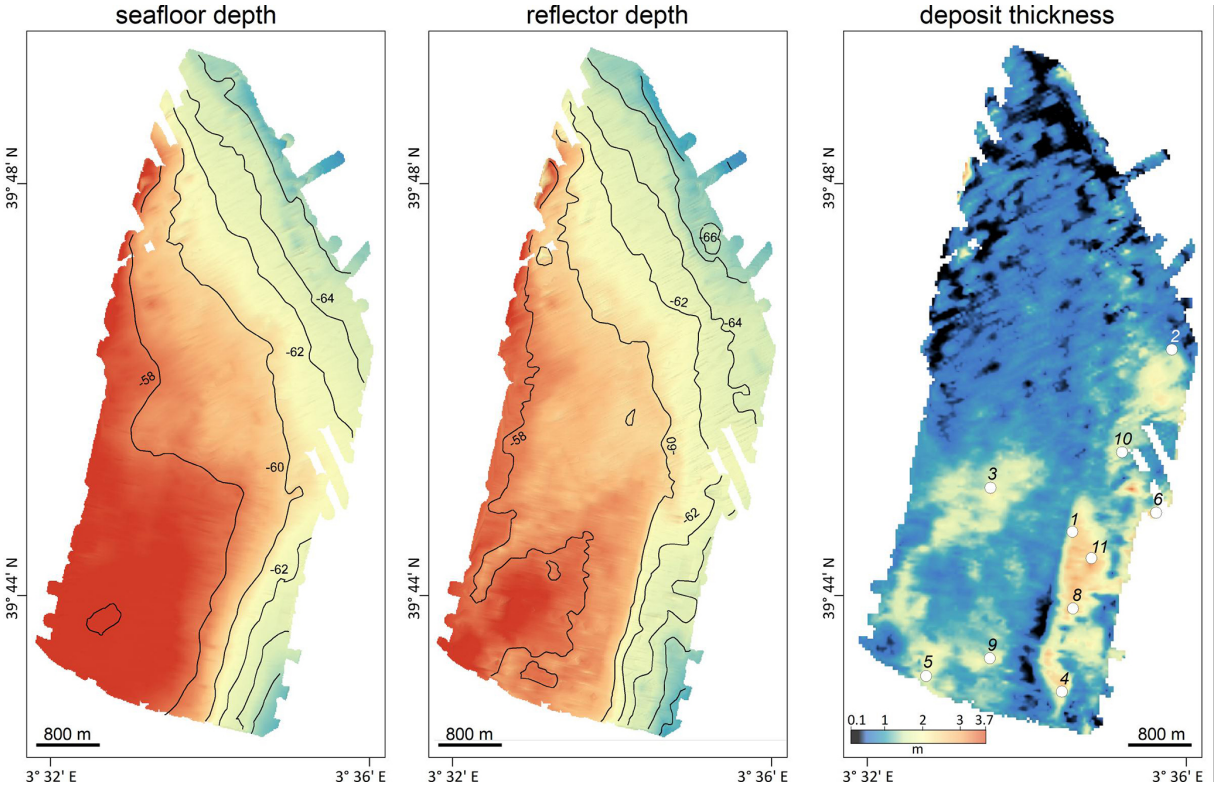

Figure 2. Results of the high-resolution profiling in the rhodolith deposit. Left panel: bathymetry, central panel: reflector depth, right panel: deposit thickness. Refer to position of geophysical survey in Fig. 1.

Table 1. Characteristics of the seven cores obtained in the Menorca Channel (Western Mediterranean) selected for this study. Description of biocenoses based on knowledge from our own video observations and previous projects (Moranta et al., 2014).

Vibrocore ID3	Longitude	Latitude	Sea bottom Depth (m)	core length (m)	analyses	biocenose
V1	3.5750	39.7419	61.91	1.60	+∗ #	rhodoliths > 75 %, with Peyssonnelia and Osmundaria
V2	3.5949	39.7700	66.22	1.40	+∗ $ #	rhodoliths > 75 %, with Laminaria
V4	3.5727	39.7177	66.08	1.80	+∗ $ #	rhodoliths > 60 %, with Osmundaria
V5	3.5456	39.7205	60.01	2.80	+∗ #	rhodoliths > 60 %, with Osmundaria
V6	3.5933	39.7477	64.52	1.90	+∗ $ #	rhodoliths > 60 %, with Laminaria
V10	3.5854	39.7572	63.28	1.45	+∗ #	rhodoliths > 90 %, with Peyssonnelia
V11	3.5794	39.7525	63.93	1.75	+∗ $ #	rhodoliths > 75 %, with Peyssonnelia

+ Lithology and clasts composition; * Granulometry and carbonates; $ Radiocarbon dating; # Organic carbon.

of the sampling design, with multiple depth subsamples collected within each sediment core. Because OC density values were positive and right-skewed, the response was log-transformed (log[CarDens]) and modelled assuming Gaussian errors. Core identity was included as a random intercept to accommodate non-independence among subsamples from the same core.

The following sediment characteristics, that were explored as candidate fixed effects, were: standardized sediment depth (cm), median grain size (d_{50}; µm), carbonate content (%), biogenic gravel content (%), and sediment type (categorical). Owing to strong collinearity between d_{50} and the sand/silt fractions ($|r| \approx 0.90$–0.96), grain-size fractions were not included in models containing d_{50}. Potential residual dependence within each corer along the depth profile was assessed by fitting models with a first-order autoregressive correlation structure, AR(1). In addition, a random-slope formulation allowing core-specific depth trends was tested using a diagonal random-effects structure (random intercept and depth slope by core, with intercept–slope covariance constrained to zero). Models were compared using Akaike Information Criteria, with maximum likelihood estimation used for model

selection and the best-supported model refitted by restricted maximum likelihood for final parameter estimation. The intraclass correlation coefficient (ICC) was calculated from variance components to quantify the proportion of variance attributable to differences among cores. All analyses were conducted in R v4.4.2.

3 Results

3.1 Seismoacoustic records

The surveyed area ranges from 57 to 68 m depth and exhibits generally smooth bathymetry, with an average slope of 0.2°. The western sector is relatively flat, gradually deepening from 57 to 60 m, while the southeast and northeast sections show narrow bathymetric edges with steeper slopes reaching 68 m (Fig. 2).

Geo-acoustic profiles allowed detailed mapping of the 3D architecture of the bioclastic deposit. Sediment thickness was highly heterogeneous at small scales, ranging from nearly 0 to several meters over spatial extents of hundreds of meters or less (Fig. 2, right panel; Fig. S2). Average thickness was 0.95 m, with a maximum of 3.7 m. Thinner deposits occurred in the northern sector (down to 10 cm), whereas thicker accumulations were found in the southern and eastern sectors, including a 2 km × 1 km patch reaching 3.7 m at its depocenter.

Cores were collected at locations of maximum sediment accumulation. Of the seven cores retained for this study, V1, V2, and V10 reached the bedrock horizon; V4, V6, and V11 fell short by 0.5–1.1 m; and V5 slightly penetrated the bedrock (∼ 1 m) (Figs. 2, 3, and S3).

3.2 Sediment characteristics

Visual inspection of the cores revealed a relatively uniform composition, dominated by fine to coarse bioclastic sand with occasional horizons of gravel or silt (Figs. 3, S4). Grain-size analysis confirmed sand as the dominant fraction (>50 %), with fines occasionally higher in certain horizons (e.g., V1: 40–90 cm; V2: 30–60 cm; V4: 25–65 cm; V6: 25–60 cm; V11: 35–65 cm), but never exceeding sand content. Gravel was always < 25 %, with the exception of V5: 40–50 cm, 50 % gravel. Carbonate contents were consistently ≥ 90 % along the cores.

Sediment composition was primarily carbonate bioclasts (75 %) and, to a lesser extent, carbonate lithoclasts (8 %), with variable contributions from siliciclastic grains. Stereomicroscope analysis allowed identification of 65 % of clasts, mainly unattached coralline red algae (26 %, branched and non-branched), bivalve fragments (22 %), gastropods (13 %), echinoid remains (4 %), foraminifera (4 %), and bryozoans (3 %). Minor groups included serpulids, ostracods, and polyplacophorans. Siliciclastic grains (17 %) were grey or white lithoclasts, distinguished by texture and lack of reaction to dilute HCl.

Coralline algae fragments occurred throughout the cores, whereas well-formed rhodoliths were confined to the upper ∼ 60 cm (except V2), occurring either scattered or densely packed, particularly in V4, V5, and V11 (Fig. 3). Three cores (V1, V2, V6) terminated on cemented substrate, including bivalve-rich hardgrounds or reworked lithoclasts.

3.2.1 Radiocarbon Dating

Radiocarbon dating of rhodoliths and bivalve shells from four cores (Table 2) yielded ten age estimates. Two basal ages (41 680 yr BP in V2 and 19 726 yr BP in V6) indicate reworked pre-Holocene material from periods when the area was in an emerged sub-aerial setting. The next four oldest dates, between 11 711 and 9096 yr BP, correspond to the end of Younger Dryas (11 711 yr BP) and the subsequent rapid sea-level rise (until 9000 yr BP), indicating that the area was a shallow marine environment (< 20 m depth) dominated by bivalves and dispersed branched rhodoliths. Some lithoclasts within these horizons indicate continental input consistent with shallow-water conditions.

Three younger ages, between 7058 and 6470 yr BP (47–52 cm depth in V2, V4, and V6), correspond to a period when the Menorca Channel was ∼ 10–15 m below present sea level, during which well-formed, densely packed rhodoliths accumulated (Fig. 3). During this interval, continental inputs diminished, maërl became abundant, and rhodolith beds consolidated, as exemplified by V4 (∼ 50 cm, 6672 yr BP). Scattered rhodolith fragments occasionally occur at greater depths, but none are found in strata older than 9096 yr BP, highlighting the onset of persistent rhodolith accumulation after postglacial transgression.

Based on these dates, sediment accretion rates range from 6.9 to 21.5 cm kyr^{-1} , with a median of 8.54 cm kyr^{-1} (Fig. 4).

3.3 Organic Carbon content

The average OC content in the upper 50 cm of sediment across all cores was 0.57 % (±0.22) (Table 3). OC content showed little variation with depth within this interval (Table S1 in the Supplement). Using these measurements, OC stocks were determined for each core. Over the first 30 cm, we estimate an average across all the cores of 19.41 (±4.42) Mg C ha^{-1} . Over the full 50 cm, we estimate an OC stock of 32 (±4.18) Mg C ha^{-1} across all the cores (Table 3).

In order to estimate annual OC accumulation, the 50 cm stock (3200 g C m^{-2}) was divided by the approximate age of the 50 cm horizon. Considering a median sediment accretion rate of 8.54 cm kyr^{-1}, annual OC accumulation is estimated at 0.546 g C m^{-2} yr^{-1}. These estimates should be treated with caution, bearing in mind that the sediment cores were extracted from the points of greatest sediment accumu-

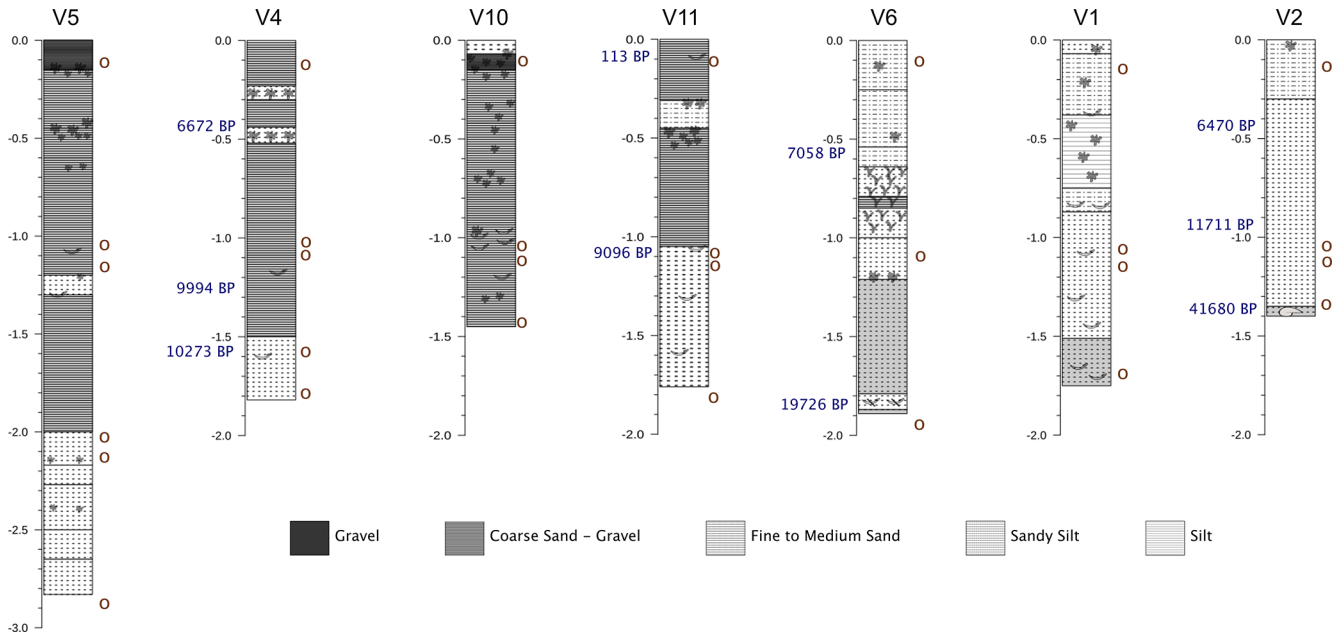

Figure 3. Stratigraphic columns showing the lithological composition of the sediment and radiocarbon dates (blue). Circles indicate samples collected for faunal identification. Clasts are illustrated according to their morphology, including branched and non-branched rhodoliths, shell fragments, and gastropod shells. Only clasts larger than 5 cm are shown.

Table 2. Radiocarbon dates (^{14}C) for carbonate bioclasts obtained from the testing laboratory of Beta Analytic (Miami, Fl., US), recalibrated with BetaCal 5.0 and corrected for the local marine reservoir effect (-112 ± 99). * Corresponds to reworked ages.

Core	Depth (cm)	Radiocarbon Date BP	Calibrated Probability Data (2σ)	Calibrated years BP
V2	136	$37\,934 \pm 875$	41 146–38315 BC 100 %	41680.5*
V2	97	$10\,490 \pm 30$	10 151–9371 BC 95.4 %	11 711
V2	47	6110 ± 30	4778–4261 BC 95.4 %	6470
V4	160.5	9460 ± 30	8640–8006 BC 95.4 %	10 273
V4	117.5	9270 ± 30	8372–7716 BC 95.4 %	9994
V4	46	6300 ± 30	5000–4444 BC 95.4 %	6672
V6	183	28067 ± 392	30 634–4918 BC 100 %	19 726*
V6	52	6552 ± 81	5298–4918 BC 100 %	7058
V11	106	8530 ± 30	7455–6837 BC 95.4 %	9096
V11	10	340 ± 30	1724–1950 BD 95.4 %	113

lation (Fig. 2). Furthermore, this also assumes a constant sediment accumulation over time and does not account for potential hiatuses or erosional activity, thus representative of a long-term historical estimate rather than flux.

The molar C / N ratios were used to assess the origin and degree of degradation of the organic matter. The average C / N ratio across all samples was 10.71 (±3.19), with the highest value being 18.51 (V11) and the lowest value being 7.71 (V4) indicating predominantly marine sources.

Mixed-effects modelling indicated that OC density in the upper 50 cm was primarily explained by carbonate content and grain size (d_{50}), with a weaker contribution from biogenic gravel content, while depth within the core showed no consistent effect. Alternative model structures, including sediment type, random slopes for depth, and AR(1) correlation across depth, did not improve model fit and were not retained (see Tables S2, S3). In the final model, d_{50} was positively associated with OC density ($\beta = 0.177$, $p = 0.0046$) and carbonate was negatively associated with OC density ($\beta = -0.306$, $p < 0.001$), whereas biogenic gravel showed a weaker positive association ($\beta = 0.098$, $p = 0.0688$) and depth was not significant ($p = 0.577$). Approximately 42 % of the variability in OC density was attributable to differences among cores, with the remaining variance occurring within cores and as unexplained residual variability (Fig. 5).

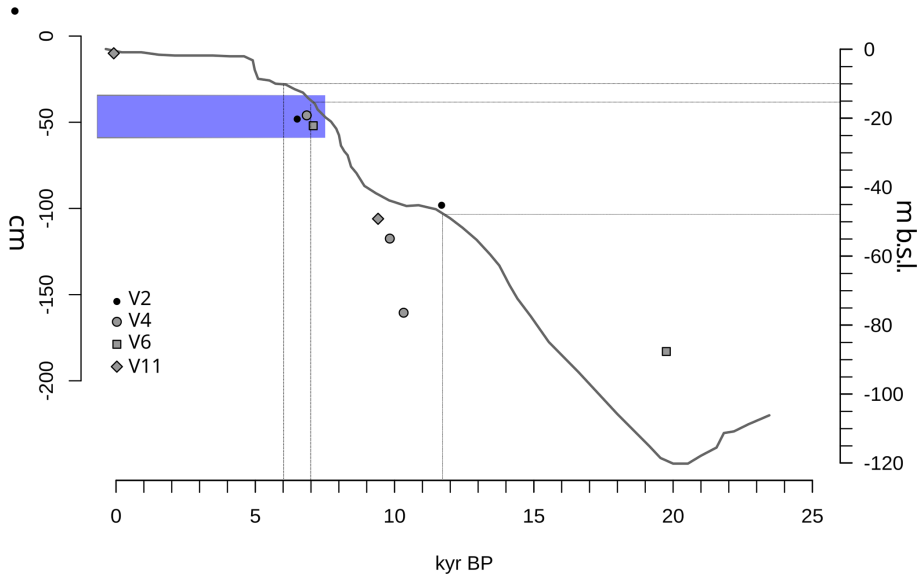

Figure 4. Age-depth plot for the dated cores (excluding one sample that yielded a date > 40 kyr BP) from the rhodolith deposit of the Menorca channel. Sea-level height (m) relative to present day based on the average model from Bianchi et al. (2012), largely based on results from Lambeck and Bard (2000). Relevant dates for this deposit (end of Younger Dryas at 11 700 yr BP and period of sea level stabilization between 7000 and 6000 yr BP) are marked along the x-axis and the corresponding depth below current sea level on the right y-axis. Blue stripe between 35 and 60 cm core depth shows the onset of horizons with high abundance of rhodoliths.

Table 3. Summary table showing the average organic carbon density, the stock over the top 30 and 50 cm of the cores.

Core	Avg C Density ($kg\ C\ m^{-3}$)	Carbon Stock Top 30 cm ($Mg\ C\ ha^{-1}$)	Carbon Stock 50 cm ($Mg\ C\ ha^{-1}$)
V1	5.87	24.28	29.36
V2	6.77	19.94	33.84
V4	7.75	14.92	38.74
V5	7.15	25.19	35.75
V6	6.54	20.68	32.72
V10	5.46	18.99	27.31
V11	5.031	11.82	26.54
All Cores	6.41	19.41	32.04

4 Discussion

The Holocene sedimentary deposit underlying the present-day rhodolith bed in the Menorca Channel reflects a highly dynamic environment shaped by post-glacial sea-level rise. The deposit rests on an erosional unconformity that likely incorporates reworked Miocene–Pliocene materials (Guillén, 1987). The pronounced spatial variability observed among corers, even over relatively short distances, suggests that local paleo-topography has exerted a strong control on sediment accumulation. Similar patterns have been reported from other temperate carbonate shelves, where interactions between seabed morphology and hydrodynamic conditions generate a complex mosaic of erosion, transport and deposition (Betzler et al., 2011; Fornós and Ahr, 1997). These processes have likely shaped the present bioclastic seascape of the Menorca Channel and contributed to the long-term persistence of rhodolith-rich habitats. Importantly, the heterogeneous distribution of sediments indicates that organic carbon storage is unlikely to be uniform across the bed. Consequently, reliable estimates of carbon stocks will require extending geophysical surveys and sediment sampling to capture this spatial variability.

Radiocarbon data suggests that rhodolith assemblages in the Menorca Channel established during the Early Holocene and developed under conditions comparable to other mid- to late-Holocene shallow marine carbonate systems. Their timing placed them between younger maërl deposits in western France (5860–5300 yr BP, Ehrhold et al., 2021) and older rhodolith beds reported from the Gulf of Mexico (13 886 yr BP, Olmstead and Andrus, 2024), although such comparisons should be interpreted cautiously given re-

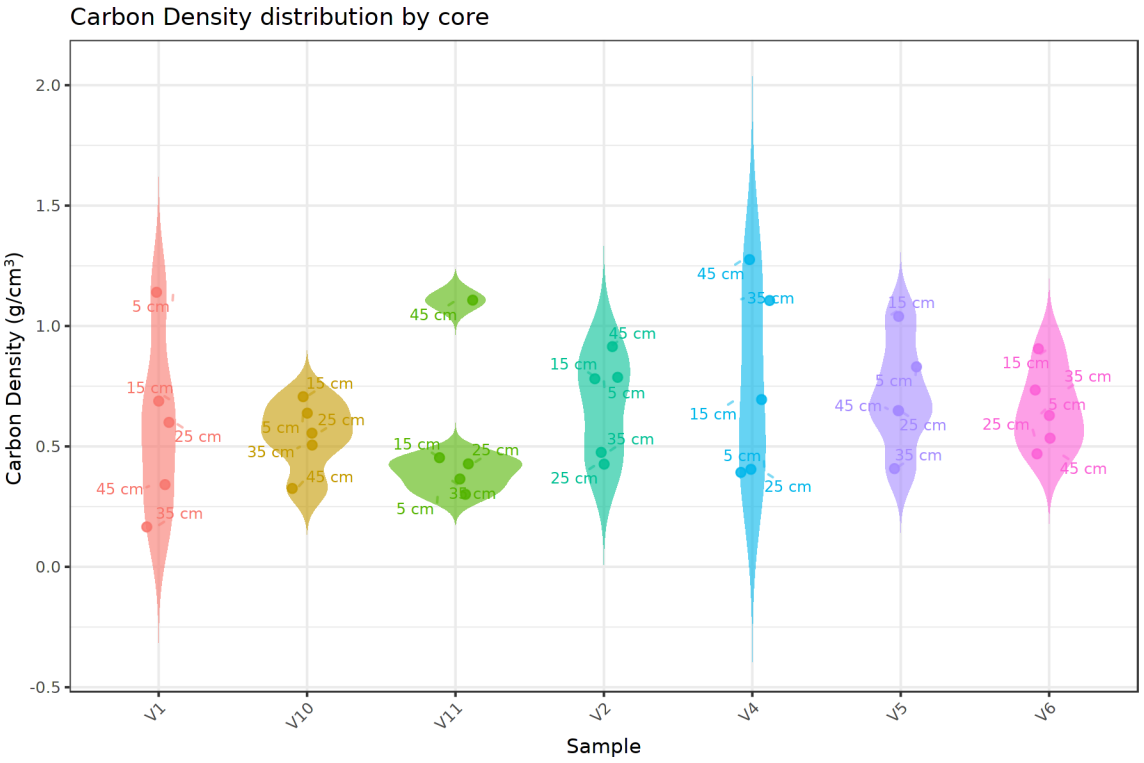

Figure 5. Organic carbon density in the sediments (g cm^{-3}) of the first 50 cm of cores.

gional differences in environmental and depositional settings. Within the Menorca Channel records, deposits formed at the end of the Younger Dryas and during rapid postglacial sea-level rise (~ 9000 yr BP onwards) are characterized by bivalves-dominated assemblages with dispersed branched rhodoliths. The interpretation of the lower and older sections of the cores is complicated by presence of reworked deposits; nevertheless, the data suggest that well-formed rhodoliths most probably established later (upper ~ 60 cm of sediment, around 7000–6000 yr BP), when more stable conditions prevailed and coincide with sea-level stabilization near present-day levels (Lambeck, 1995). This transition marks the onset of dense rhodolith beds characterised by large, tightly packed rhodoliths, with branched and boxwork morphologies, whose expansion and long-term persistence were likely favored by moderate hydrodynamics, reduced terrigenous input, and mesophotic conditions that limit competitive pressure (Aguirre et al., 2012; Basso et al., 2017). This continued presence over 6000 years highlights the capacity of these systems to maintain structural complexity in the long-term, with potential implications for their role as long-term organic carbon deposits, and for their conservation and management.

Present-day seafloor patterns in the Menorca Channel are characterized by patches of rhodoliths occurring at high densities (50 %–100 % surface coverage), ranging in size from ~ 10 to over 100 m^2, and predominantly composed of branched forms (Cabrito et al., 2024a, b). This spatial heterogeneity is consistent with observations from other deep Mediterranean rhodolith beds (Rendina et al., 2020; Bracchi et al., 2022; Tabone et al., 2024). Sediments are consistently carbonate-rich and dominated by bioclastic material, with relatively uniform organic carbon content in the upper layers. In contrast, sediment thickness is highly heterogeneous at small spatial scales. Reflecting these patterns, mixed-effects modelling indicated that approximately 42 % of the variability in organic carbon density was attributable to differences among cores, suggesting small-scale patchiness in carbon accumulation across the rhodolith bed that may be linked to local patchiness in rhodolith morphology and accumulation. Spatial heterogeneity, together with variability in rhodolith density and morphology, may influence particle trapping capacity and organic carbon retention (Cabrito et al., 2024a; Neto et al., 2021); however, this remains to be evaluated, as the cores analysed were collected in the deepest sediment deposits from the main rhodolith patch characterized by high cover and structural complexity. Organic carbon density was largely controlled by sediment composition (grain size and carbonate content), consistent with dilution in carbonate-rich sediments and a textural control on carbon storage (Howard et al., 2018; Keil et al., 1994). The absence of a depth effect suggests relatively uniform near-surface conditions, consistent with active bioturbation and hydrodynamic reworking that promote sediment mixing.

The relatively uniform organic carbon content in the upper 50 cm of sediment suggests low degradation rates over the last ∼6000 years, coinciding with sea level stabilization. This stability likely favored the development of well-formed rhodolith ecosystems, facilitating organic carbon capture and long-term retention. Based on our estimates, these sediments store approximately 32.04 Mg C ha^{-1} in the upper 50 cm, with an average of 19.41 (±4.42) Mg C ha^{-1} in the upper 30 cm. Using an estimated sediment accretion rate of 8.54 cm kyr^{-1}, this corresponds to an average organic carbon accumulation of ∼0.546 g C m^{-2} yr^{-1}. These values exceed previous estimates reported for coralline algal beds in temperate coastal environments. For example, Mao et al. (2020) reported average organic carbon stocks of 7.23 ± 1.30 Mg C ha^{-1} within the upper 25 cm and 12.28 ± 1.98 Mg C ha^{-1} across the full depth of carbonate deposits (∼80 cm) in Scottish coastal rhodolith beds. The substantially higher carbon stocks observed in the Menorca deposit likely reflect differences in the environmental context: extending to mesophotic depths it allows long-term depositional stability and slow sediment turnover. Rather than acting as a rapid carbon sink, this system would serve as a millennial-scale carbon reservoir, preserving organic matter within a slowly forming carbonate matrix. Nevertheless, future work should investigate deeper sediment layers (>50 cm), to determine the depth and age at which organic carbon mineralized. This would also help to clarify the role of spatial heterogeneity in the deposit, and whether areas with thinner sediment cover differ in their capacity for carbon retention.

The relatively high organic carbon stocks documented in the Menorca Channel reinforce growing evidence that rhodolith beds can contribute to long-term carbon storage despite slow sediment accretion rates (Mao et al., 2024; van der Heijden and Kamenos, 2015). The persistence of organic carbon observed in these deposits reflects two complementary processes: the long-term preservation of organic matter within slowly accumulating sediments and the longevity of coralline algal systems, whose carbonate skeletons resist degradation and maintain biogenic habitats over millennial timescales (Aguirre et al., 2000; van der Heijden and Kamenos, 2015; Wilson et al., 2004). The three-dimensional structure of rhodolith beds promotes the trapping and burial of suspended organic matter, including allochthonous carbon, while low remineralization rates favour its preservation over long timescales (James et al., 2024). While rhodolith beds can store substantial amounts of organic carbon, their net contribution to climate mitigation remains an open question because the balance between carbon burial and calcification-related carbon release is not yet fully resolved (Kamenos et al., 2013; Mao et al., 2024; Schubert et al., 2024; van der Heijden and Kamenos, 2015).Within this context, Blue Carbon frameworks have focused on mangroves, salt marshes, and seagrass meadows. However, coralline algal beds are increasingly recognized as non-classical Blue Carbon ecosystems because of their capacity to store organic carbon over centennial to millennial timescales (James et al., 2024). While their annual accumulation rates are relatively low, their extensive global distribution and long-term persistence suggest that their cumulative contribution to coastal carbon storage may be substantial (van der Heijden and Kamenos, 2015). The carbon stocks quantified in the Menorca Channel support this emerging perspective and highlight the importance of protecting these ecosystems, as disturbance can rapidly mobilize carbon deposits that have accumulated over millennia.

These ecosystems are highly vulnerable to physical disturbance, particularly from bottom-contact fishing such as trawling and dredging (Trégarot et al., 2024). These activities can fragment nodules, bury living rhodoliths, and alter the structure and compaction of the sediment, with impacts that persist over timescales far longer than ecosystem management schemes (de Juan et al., 2013; Cabanellas-Reboredo et al., 2018; Tauran et al., 2020). The upper few centimeters of the deposit can be disrupted by a single trawl passage, not only halting carbon sequestration but potentially remobilizing organic carbon that accumulated over thousands of years (Bernard et al., 2019). In the Mediterranean, many rhodolith beds remain exposed to such pressures, as they alternate with soft-sediment ecosystems exposed to commercial trawling (de Juan et al., 2013; Illa-López et al., 2023). In contrast, the Menorca Channel deposit has been protected from trawling due to the historical presence of submarine cables. Evidence from this less disturbed site suggests relatively uniform carbon preservation and burial under natural, undisturbed conditions. This evidence highlights the need for future research into rhodolith beds. In particular, this would include assessing whether organic carbon trapped by rhodolith beds, as opposed to carbon produced via rhodolith calcification, is sequestered at rates that balanced or exceed calcification-related carbon release. This highlights the critical role of protection in maintaining the long-term carbon storage and ecological integrity of rhodolith ecosystems.

5 Conclusions

Rhodolith beds in the western Menorca Channel form the surficial sedimentary layer over a Holocene depositional framework and constitute long-term sedimentary carbon archives within carbonate shelf systems. Their organic carbon content remains relatively stable through the upper 50 cm, indicating sustained accumulation and limited degradation over ∼6000 years. This persistence is enabled by the three-dimensional structure of rhodoliths, which promotes sediment trapping and long-term carbon preservation despite slow accretion rates, supporting their role as long-term carbon reservoirs rather than rapid carbon sinks. These systems have persisted despite environmental changes, including human impacts, yet their slow growth and sensitivity

to physical disturbance make them highly vulnerable. Protecting rhodolith beds from trawling and dredging is essential not only for biodiversity conservation but also for maintaining their function as long-term carbon stores, reinforcing their contribution to climate regulation. These findings suggest that carbonate biogenic systems such as rhodolith beds should be reconsidered as long-term carbon repositories within blue carbon frameworks.

Data availability. The data supporting the findings of this study, including sediment core descriptions, geochemical analyses, and radiocarbon dates, are available from the corresponding author upon reasonable request.

Supplement. The supplement related to this article is available online at https://doi.org/10.5194/bg-23-4779-2026-supplement.

Author contributions. SdJ, FM, and CL conceptualized the study. AC, MdMG, SdJ, RS, and LI conducted sample collection and processing. MdMG and CL curated the data. SdJ, RS, and AO performed the formal analysis. CL, RS, and AO developed the methodology. SdJ, FM, and CL prepared the original draft of the manuscript. HH, JG, and GC contributed to reviewing and editing the manuscript. SdJ, FM, and GC acquired funding.

Competing interests. The contact author has declared that none of the authors has any competing interests.

Disclaimer. Publisher's note: Copernicus Publications remains neutral with regard to jurisdictional claims made in the text, published maps, institutional affiliations, or any other geographical representation in this paper. The authors bear the ultimate responsibility for providing appropriate place names. Views expressed in the text are those of the authors and do not necessarily reflect the views of the publisher.

Acknowledgements. The authors would like to thank the crew of the R/V *SOCIB* and R/V *Sarmiento de Gamboa* during the research cruises, partly funded by the Spanish Ministry of Science and Innovation. We thank the companies NAUTILUS and GEOMYTSA for their technical support during field work to obtain geophysical maps and vibrocores.

Financial support. This work was funded by EU Horizon project MARBEFES (HORIZON-CL6-2021-BIODIV-01 Theme, Grant Agreement no. 101060937) and RHODOMED (Spanish Ministry of Science grant no. PID2023-146998OB-C22). This work contributes to IMEDEA's "Center of Excellence" Maria de Maetzu (CEX2021-001198) and ICM's "Center of Excellence" Severo Ochoa (CEX2019-000928-5). The Spanish Ministry of Science and Innovation supported S.d.J. with a "Ramón y Cajal" grant (RyC2020-029062-I), A.O.-A. with a "Ramon y Cajal" grant (RyC2023–043454-I) and L.I.-L with a FPI predoctoral (PRE2022-104567).

The article processing charges for this open-access publication were covered in part by the CSIC Open Access Publication Support Initiative through its Unit of Information Resources for Research (URICI).

Review statement. This paper was edited by Niels de Winter and reviewed by two anonymous referees.

References

Aguirre, J., Riding, R., and Braga, J. C.: Diversity of coralline red algae: origination and extinction patterns from the Early Cretaceous to the Pleistocene, Paleobiology, 26, 651–667, https://doi.org/10.1666/0094-8373(2000)026<0651:DOCRAO>2.0.CO;2, 2000.

Aguirre, J., Braga, J. C., MArtín, J. M., and Betzler, C.: Palaeoenvironmental and stratigraphic significance of Pliocene rhodolith beds and coralline algal bioconstructions from the Carboneras Basin (SE Spain), Geodiversitas, 34, 115–136, https://doi.org/10.5252/g2012n1a7, 2012.

Aguirre, J., Braga, J. C., and Bassi, D.: Rhodoliths and rhodolith beds in the rock record, in: Rhodolith/maërl beds: A global perspective, Springer, 105–138, https://doi.org/10.1007/978-3-319-29315-8_5, 2017.

Alonso, B., Guillén, J., Canals, M., Serra, J., Acosta, J., Herranz, P., Sanz, J. L., Calafat, A., and CATAFAU, A.: Los sedimentos de la plataforma continental balear, Acta Geológica Hispánica, 185–196, 1988.

Amado-Filho, G. M., Moura, R. L., Bastos, A. C., Salgado, L. T., Sumida, P. Y., Guth, A. Z., Francini-Filho, R. B., Pereira-Filho, G. H., Abrantes, D. P., Brasileiro, P. S., Bahia, R. G., Leal, R. N., Kaufman, L., Kleypas, J. A., Farina, M., and Thompson, F. L.: Rhodolith beds are major $CaCO_3$ bio-factories in the tropical South West Atlantic, PloS ONE, 7, e35171, https://doi.org/10.1371/journal.pone.0035171, 2012.

Barbier, E. B., Hacker, S. D., Kennedy, C. J., Koch, E. W., Stier, A. C., and Silliman, B. R.: The value of estuarine and coastal ecosystem services, Ecol. Monogr., 81, 169–193, https://doi.org/10.1890/10-1510.1, 2011.

Basso, D.: Deep rhodolith distribution in the Pontian Islands, Italy: a model for the paleoecology of a temperate sea, Palaeogeogr. palaeocl., 137, 173–187, https://doi.org/10.1016/S0031-0182(97)00099-0, 1998.

Basso, D., Caragnano, A., Benzoni, F., and Rodondi, G.: Southern Sinai rhodoliths: facies, species composition, and growth rate (Red Sea, Egypt), in: International rhodolith workshop, https://d1wqtxts1xzle7.cloudfront.net/66486527/Abstract_20volume-WEB-libre.pdf (last access: 3 July 2026), 2012.

Basso, D., Babbini, L., Ramos-Esplá, A. A., and Salomidi, M.: Mediterranean rhodolith beds, Rhodolith/Maërl Beds: a global perspective, Coastal Research Library, vol. 15, Springer, Cham, 281–298, https://doi.org/10.1007/978-3-319-29315-8_11, 2017.

Bernard, G., Romero-Ramirez, A., Tauran, A., Pantalos, M., Deflandre, B., Grall, J., and Grémare, A.: Declining maerl vitality and habitat complexity across a dredging gradient: insights from in situ sediment profile imagery (SPI), Sci. Rep., 9, 16463, https://doi.org/10.1038/s41598-019-52586-8, 2019.

Betzler, C., Braga, J. C., Jaramillo-Vogel, D., Roemer, M., Huebscher, C., Schmiedl, G., and Lindhorst, S.: Late Pleistocene and Holocene cool-water carbonates of the Western Mediterranean Sea, Sedimentology, 58, 643–669, https://doi.org/10.1111/j.1365-3091.2010.01177.x, 2011.

Bianchi, C. N., Morri, C., Chiantore, M., Montefalcone, M., Parravicini, V., and Rovere, A.: Mediterranean Sea Biodiversity Between the Legacy from the Past and a Future of Change, in: Life in the Mediterranean Sea: A Look at Habitat Changes, Nova Science, New York, 1–55 https://www.researchgate.net/publication/242397422 (last access: 3 July 2026), 2012.

Bosence, D. W.: The occurrence and ecology of recent rhodoliths – a review, Coated grains, 225–242, https://doi.org/10.1007/978-3-642-68869-0_20, 1983.

Bracchi, V. A., Caronni, S., Meroni, A. N., Burguett, E. G., Atzori, F., Cadoni, N., Marchese, F., and Basso, D.: Morphostructural characterization of the heterogeneous rhodolith bed at the marine protected area "capo carbonara" (Italy) and hydrodynamics, Diversity, 14, 51, https://doi.org/10.3390/d14010051, 2022.

Bulleri, F., Schubert, N., Hall-Spencer, J., Basso, D., Burdett, H., Francini-Filho, R., Grall, J., Horta, P., Kamenos, N., Martin, S., Nannini, M., Neves, P., Olivé, I., Peña, V., Ragazzola, F., Ribeiro, C., Rinde, E., Sissini, M., Tuya, F., and Silva, J.: Positive species interactions structure rhodolith bed communities at a global scale, Biol. Rev., 100, 428–444, https://doi.org/10.1111/brv.13148, 2025.

Cabanellas-Reboredo, M., Mallol, S., Barberá, C., Vergés, A., Díaz, D., and Goñi, R.: Morpho-demographic traits of two maërl-forming algae in beds with different depths and fishing histories., Aquat. Conserv., 28, https://doi.org/10.1002/aqc.2827, 2018.

Cabrito, A., de Juan, S., Hinz, H., and Maynou, F.: Morphological insights into the three-dimensional complexity of rhodolith beds, Mar. Biol., 171, 127, https://doi.org/10.1007/s00227-024-04437-y, 2024a.

Cabrito, A., Maynou, F., Simide, R., Mouillot, D., Lossent, J., and de Juan, S.: Non-extractive fish diversity assessment in Mediterranean rhodolith beds, Aquat. Conserv., 34, e4212, https://doi.org/10.1002/aqc.4212, 2024b.

Canals, M. and Ballesteros, E.: Production of carbonate particles by phytobenthic communities on the Mallorca-Menorca shelf, northwestern Mediterranean Sea, Deep-Sea Res. Pt. II, 44, 611–629, https://doi.org/10.1016/S0967-0645(96)00095-1, 1997.

de Juan, S., Lo Iacono, C., and Demestre, M.: Benthic habitat characterisation of soft-bottom continental shelves: Integration of acoustic surveys, benthic samples and trawling disturbance intensity, Estuar. Coast. Shelf S., 117, 199–209, https://doi.org/10.1016/j.ecss.2012.11.012, 2013.

de Juan, S., Ospina-Alvarez, A., Hinz, H., Moranta, J., and Barberá, C.: The continental shelf seascape: a network of species and habitats, Biodivers. Conserv., 1–20, https://doi.org/10.1007/s10531-023-02552-8, 2023.

Ehrhold, A., Jouet, G., Le Roy, P., Jorry, S. J., Grall, J., Reixach, T., Lambert, C., Gregoire, G., Goslin, J., Roubi, A., Penaud, A., Vidal, M., and Siano, R.: Fossil maerl beds as coastal indicators of late Holocene palaeo-environmental evolution in the Bay of Brest (Western France), Palaeogeogr. Palaeocl., 577, 110525, https://doi.org/10.1016/j.palaeo.2021.110525, 2021.

de Macêdo Carneiro, P. B., de Lima, J. P., Bandeira, Ê. V. P., Neto, A. R. X., Barreira, C. de A. R., de Souza Tâmega, F. T., Matthews-Cascon, H., Junior, W. F., and de Morais, J. O.: Structure, growth and $CaCO_3$ production in a shallow rhodolith bed from a highly energetic siliciclastic-carbonate coast in the equatorial SW Atlantic Ocean, Mar. Environ. Res., 166, 105280, https://doi.org/10.1016/j.marenvres.2021.105280, 2021.

Fornós, J. J. and Ahr, W.: Temperate carbonates on a modern, low-energy, isolated ramp; the Balearic platform, Spain, J. Sediment. Res., 67, 364–373, https://doi.org/10.1306/D4268572-2B26-11D7-8648000102C1865D, 1997.

Guillén, J.: La sedimentación carbonatada en la plataforma continental de Campos (Sur de Mallorca), University of Barcelona, http://hdl.handle.net/10261/154537 (last access: 3 July 2026), 1987.

Howard, J. L., Creed, J. C., Aguiar, M. V., and Fourqurean, J. W.: CO_2 released by carbonate sediment production in some coastal areas may offset the benefits of seagrass "Blue Carbon" storage, Limnol. Oceanogr., 63, 160–172, https://doi.org/10.1002/lno.10621, 2018.

Illa-López, L., Cabrito, A., de Juan, S., Maynou, F., and Demestre, M.: Distribution of rhodolith beds and their functional biodiversity characterisation using ROV images in the western Mediterranean Sea, Sci. Total Environ., 905, 167270, https://doi.org/10.1016/j.scitotenv.2023.167270, 2023.

James, K., Macreadie, P. I., Burdett, H. L., Davies, I., and Kamenos, N. A.: It's time to broaden what we consider a 'blue carbon ecosystem', Glob. Change Biol., 30, e17261, https://doi.org/10.1111/gcb.17261, 2024.

Jardim, V., Grall, J., Barros-Barreto, B., Bizien, A., Benoit, T., Braga, J.. Brodie, J., Burel, T., Cabrito, A., Diaz-Pulido, G., Gagnon, P., Hall-Spencer, J., Helias, M., Antunes Horta, P., Joshi, S., Kamenos, N., Kolzenburg, R., Krieger, E., Legrand, E., Page, T., Peña, V., Ragazzola, F., Rasmusson, L., Rendina, F., Schubert, N., Silva, J., Tâmega, F., Tauran, A., and Burdett, H.: A common terminology to unify research and conservation of coralline algae and the habitats they create, Aquat. Conserv., 35, e70121, https://doi.org/10.1002/aqc.70121, 2025.

Joher, S., Ballesteros, E., and Rodríguez-Prieto, C.: Macroalgal-dominated coastal detritic communities from the Western Mediterranean and the Northeastern Atlantic, Mediterr. Mar. Sci., 17, 476–495, https://doi.org/10.12681/mms.1438, 2016.

Kamenos, N. A., Burdett, H. L., Aloisio, E., Findlay, H. S., Martin, S., Longbone, C., Dunn, J., Widdicombe, S., and Calosi, P.: Coralline algal structure is more sensitive to rate, rather than the magnitude, of ocean acidification, Glob. Change Biol., 19, 3621–3628, https://doi.org/10.1111/gcb.12351, 2013.

Keil, R. G., Tsamakis, E., Fuh, C. B., Giddings, J. C., and Hedges, J. I.: Mineralogical and textural controls on the organic composition of coastal marine sediments: Hydrodynamic separation using SPLITT-fractionation, Geochim. Cosmochim. Ac., 58, 879–893, https://doi.org/10.1016/0016-7037(94)90512-6, 1994.

Lambeck, K.: Late Pleistocene and Holocene sea-level change in Greece and south-western Turkey: a separation of eustatic, isostatic and tectonic contributions, Geophys. J. Int., 122, 1022–

1044, https://doi.org/10.1111/j.1365-246X.1995.tb06853.x, 1995.

Lambeck, K. and Bard, E.: Sea-level change along the French Mediterranean coast for the past 30 000 years, Earth Planet. Sc. Lett., 175, 203–222, https://doi.org/10.1016/S0012-821X(99)00289-7, 2000.

Lo Iacono, C., Mateo, M. A., Gracia, E., Guasch, L., Carbonell, R., Serrano, L., Serrano, O., and Danobeitia, J.: Very high-resolution seismo-acoustic imaging of seagrass meadows (Mediterranean Sea): Implications for carbon sink estimates, Geophys. Res. Lett., 35, https://doi.org/10.1029/2008GL034773, 2008.

Macreadie, P., Anton, A., Raven, J., Beaumont, N., Connolly, R., Friess, D., Kelleway, J., Kennedy, H., Kuwae, T., Lavery, P., Lovelock, C., Smale, D., Apostolaki, E., Atwood, T., Baldock, J., Bianchi, T., Chmura, G., Eyre, B., Fourqurean, J., Hall-Spencer, J., Huxham, M., Hendriks, I., Krause-Jensen, D., Laffoley, D., Luisetti, T., Marbà, N., Masque, P., McGlathery, K., Megonigal, P., Murdiyarso, D., Russell, B., Santos, R., Serrano, O., Silliman, B., Watanabe, K., and Duarte, C.: The future of Blue Carbon science, Nat. Commun., 10, 3998, https://doi.org/10.1038/s41467-019-11693-w, 2019.

Mao, J., Burdett, H. L., McGill, R. A., Newton, J., Gulliver, P., and Kamenos, N. A.: Carbon burial over the last four millennia is regulated by both climatic and land use change, Glob. Change Biol., 26, 2496–2504, https://doi.org/10.1111/gcb.15021, 2020.

Mao, J., Burdett, H., and Kamenos, N.: Efficient carbon recycling between calcification and photosynthesis in red coralline algae, Biol. Lett., 20, https://doi.org/10.1098/rsbl.2023.0598, 2024.

Middelburg, J. J.: Reviews and syntheses: to the bottom of carbon processing at the seafloor, Biogeosciences, 15, 413–427, https://doi.org/10.5194/bg-15-413-2018, 2018.

Moranta, J., Barberá, C., Druet, M., and Zaragoza, N.: Caracterización ecológica de la plataforma continental (50–100 m) del canal de Menorca. Informe final área LIFE+ INDEMARES (LIFE07/NAT/E/000732), Instituto Español de Oceanografía-Centro Oceanográfico de Baleares, Palma, https://digital.csic.es/handle/10261/318214 (last access 3 July 2026), 2014.

Nellemann, C., Corcoran, E., Duarte, C., Valdes, L., DeYoung, C., Fonseca, L., and Grimsditch, G., (Eds.): Blue Carbon: The Role of Healthy Oceans in Binding Carbon, United Nations Environmental Programme, GRID-Arendal, https://gridarendal-website-live.s3.amazonaws.com/production/documents/:s_document/83/original/BlueCarbon_screen.pdf?1483646492 (last access: 3 July 2026), 2009.

Neto, J. M., Bernardino, A. F., and Netto, S. A.: Rhodolith density influences sedimentary organic matter quantity and biochemical composition, and nematode diversity, Mar. Environ. Res., 171, 105470, https://doi.org/10.1016/j.marenvres.2021.105470, 2021.

Olmstead, S. A. and Andrus, C. F. T.: Growth characterization of mesophotic rhodoliths in the northern Gulf of Mexico using radiocarbon dating, Palaeogeogr. Palaeocl., 654, 112438, https://doi.org/10.1016/j.palaeo.2024.112438, 2024.

Rendina, F., Kaleb, S., Caragnano, A., Ferrigno, F., Appolloni, L., Donnarumma, L., Russo, G. F., Sandulli, R., Roviello, V., and Falace, A.: Distribution and characterization of deep rhodolith beds off the Campania coast (SW Italy, Mediterranean Sea), Plants, 9, 985, https://doi.org/10.3390/plants9080985, 2020.

Rendina, F., Donnarumma, L., Ferrigno, F., and Russo, G. F.: Biodiversity of Mediterranean mesophotic rhodolith beds: Macrofaunal community composition and structure (SW Italy), Cont. Shelf Res., 105682, https://doi.org/10.1016/j.csr.2026.105682, 2026.

Riosmena-Rodríguez, R., Nelson, W., and Aguirre, J.: Rhodolith/maërl beds: a global perspective, Springer, https://doi.org/10.1007/978-3-319-29315-8, 2017.

Schubert, N., Tuya, F., Peña, V., Horta, P., Salazar, V., Neves, P., Ribeiro, C., Otero-Ferrer, F., Espino, F., Schoenrock, K., Ragazzola, F., Olivé, I., Giaccone, T., Nannini, M., Mangano, C., Sará, G., Mancuso, F., Tantillo, M., Bosch-Belmar, M., Martin, S., Le Gall, L., Santos, R., and Silva, J.: "Pink power" – the importance of coralline algal beds in the oceanic carbon cycle, Nat. Commun., 15, 8282, https://doi.org/10.1038/s41467-024-52697-5, 2024.

Tabone, L., Knittweis, L., Aguilar, R., Alvarez, H., Borg, J. A., Garcia, S., Schembri, P. J., and Evans, J.: Habitat characterization, anthropogenic impacts and conservation of rhodolith beds off southeastern Malta, Aquat. Conserv., 34, e4148, https://doi.org/10.1002/aqc.4148, 2024.

Tauran, A., Dubreuil, J., Guyonnet, B., and Grall, J.: Impact of fishing gears and fishing intensities on maerl beds: An experimental approach, J. Exp. Mar. Biol. Ecol., 533, 151472, https://doi.org/10.1016/j.jembe.2020.151472, 2020.

Teichert, S.: Attached and free-living crustose coralline algae and their functional traits in the geological record and today, Facies, 70, 8, https://doi.org/10.1007/s10347-024-00682-1, 2024.

Trégarot, E., D'Olivo, J.P., Botelho, A., Cabrito, A., Cardoso, G., Casal, G., Cornet, C., Cragg, S., Degia, K., Fredriksen, S., Furlan, E, Heiss, G., Kersting, D., Maréchal, J.P., Meesters, E., O'Leary, B., Pérez, G., Seijo-Núñez, C., Simide, R., van der Geest, M., and de Juan, S.: Effects of climate change on marine coastal ecosystems – A review to guide research and management, Biol. Conserv., 289, 110394, https://doi.org/10.1016/j.biocon.2023.110394, 2024.

Tuya, F., Schubert, N., Aguirre, J., Basso, D., Bastos, E., Berchez, F., Bernardino, A., Bosch, N., Burdett, H., Espino, F., Fernández-Gárcia, C., Francini-Filho, R., Gagnon, P., Hall-Spencer, J., Haroun, R., Hofmann, L., Horta, P., Kamenos, N., Le Gall, L., Magris., R., and Tâmega, F.: Levelling-up rhodolith-bed science to address global-scale conservation challenges, Sci. Total Environ., 164818, https://doi.org/10.1016/j.scitotenv.2023.164818, 2023.

UNEP-MAP-RAC/SPA: Action Plan for the Conservation of the Coralligenous and Other Calcareous Bio-concretions in the Mediterranean Sea, RAC/SPA, Tunis, 21 pp., https://www.rac-spa.org/sites/default/files/action_plans/pacoralligene.pdf (last access: 3 July 2026), 2008.

van der Heijden, L. H. and Kamenos, N. A.: Reviews and syntheses: Calculating the global contribution of coralline algae to total carbon burial, Biogeosciences, 12, 6429–6441, https://doi.org/10.5194/bg-12-6429-2015, 2015.

Wilson, S., Blake, C., Berges, J. A., and Maggs, C. A.: Environmental tolerances of free-living coralline algae (maerl): implications for European marine conservation, Biol. Conserv., 120, 279–289, https://doi.org/10.1016/j.biocon.2004.03.001, 2004.